UCRL-52304

COMPRESSIBLE FLUID FLOW THROUGH ROCKS OF VARIABLE PERMEABILITY

W. Lin

July 25, 1977

Prepared for U.S. Energy Research & Development Administration under contract No. W-7405-Eng-4

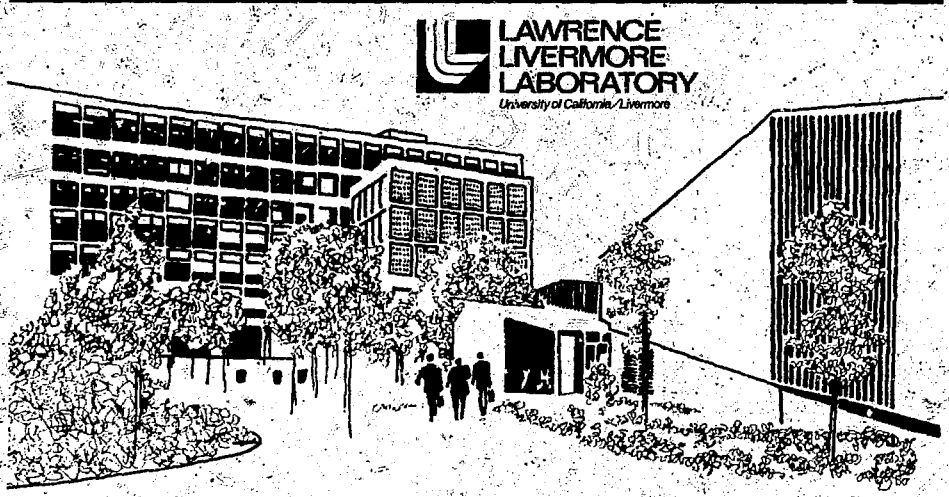

Distribution Categories
UC-70

LAWRENCE LIVERMORE LABORATORY
University of California/Livermore, California/94550

UCRL-52304

COMPRESSIBLE FLUID FLOW THROUGH ROCKS OF VARIABLE PERMEABILITY

W. Lin

MS. date: July 25, 1977

Contents

COMPRESSIBLE FLUID FLOW THROUGH ROCKS OF VARIABLE PERMEABILITY

Abstract

The effectiveness of course-grained igneous rocks as shelters for burying radioactive waste can be assessed by determining the rock permeabilities at their *in situ* pressures and stresses. We used analytical and numerical methods to solve differential equations of one-dimensional fluid flow through rocks with permeabilities from 10^4 to 1 nD. In these calculations, we used upstream and downstream reservoir volumes of 5, 50 and 500 cm^3. The optimal size combinations of the two reservoirs were determined for measurements of permeability, stress, strain, acoustic velocity, and electrical conductivity on low-porosity, coarse-grained igneous rocks.

Introduction

Successful permanent storage of solidified, highly radioactive waste requires that it be secured and shielded in a stable environment away from circulating groundwater. In many areas of the U.S. and world, coarse-grained igneous rocks (ranging from syenites to gabbros) 1 to 3 km deep may provide adequate protection for radioactive waste. Before we can accurately assess the efficiency of these rocks as waste repositories, we must first know their permeabilities at the lithostatic pressures and stress fields at such depths. To study this, we have begun a laboratory program to measure permeabilities of igneous rocks at their expected *in situ* conditions. Since we expect that the permeabilities of igneous rocks may range widely (1 to 10^{10} nD), we will need sophisticated measuring methods. Although permeabilities from 10^4 to 10^{10} nD can be determined directly from measurements of fluid flows and pressure drops across rock samples, permeabilities from 1 to 10^5 nD will be determined by the use of transient methods. Accurate measurements with such methods require, among other determinations, precise sizing of upstream and downstream reservoirs; in turn, the determination of these volumes requires the solution of one-dimensional compressible flow equations. In this

report, we evaluate these equations and describe our design of reservoir volumes for the rock and fluids we will use in our program.

Mathematical Model

To simplify our experimental analysis, we have made the following assumptions: first, the rock sample is homogeneous and isotropic, second, the flow of fluid is in one direction only, along the length of the sample, and third, the compressibility and porosity of the rock sample and the viscosity and compressibility of the fluid (water) are constant during the experiment. The third assumption is valid only when the pressure increment (Δp) is a few percent of the initial pore pressure in the sample (Brace et al.).[1]

A typical experimental configuration is schematically illustrated in Fig. 1. The flow of water is in the positive x direction. Following Darcy's law and the law of conservation of mass, the pore pressure in the sample varies as a function of distance x and time t according to the partial differential equation

$$\frac{\partial^2 p}{\partial x^2} = a^2 \frac{\partial p}{\partial t} \quad , \qquad (1)$$

for $t > 0$ and $0 < x < L$

with the boundary, initial, and final conditions[2]:

$$\frac{\partial p}{\partial x} = \lambda_1 \frac{\partial p}{\partial t} \quad , \qquad (2a)$$

for $t > 0$ and $x = 0$,

$$\frac{\partial p}{\partial x} = \lambda_2 \frac{\partial p}{\partial t} \quad , \qquad (2b)$$

for $t > 0$ and $x = L$.

$$p(0,0) = p_i \quad ,$$

$$p(x,0) = p_0 \quad ,$$

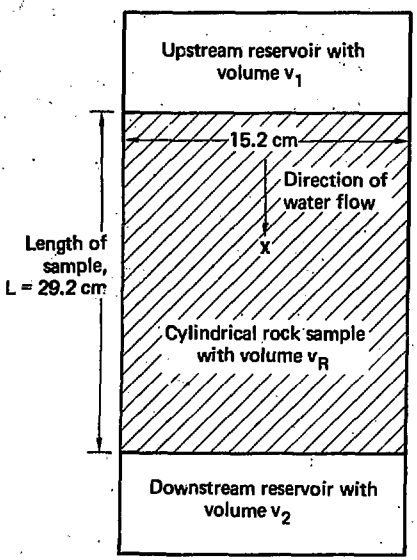

Fig. 1. Schematic diagram of the rock sample and experimental setup.

and

$$p(x,\infty) = p_0 + \frac{\Delta p\, v_1}{v_1 + v_2 + \phi v_R} ,$$

where $\Delta p = p_1 - p_0$.

The coefficients in these equations are

$$a^2 = \frac{\mu}{k}\left[\phi\beta + \beta_{eff} - \beta_s(1+\phi)\right] ,$$

$$\lambda_1 = \frac{\mu v_1 \beta}{Ak} ,$$

$$\lambda_2 = \frac{\mu v_2 \beta}{Ak} ,$$

where μ and β are the viscosity and compressibility of water, β_{eff} and β_s are the compressibility of the whole rock and its solid matrix, and k, ϕ, and A are the permeability, porosity, and cross-section area of the sample, respectively.

PREVIOUS STUDIES

Brace et al.[1] measured the permeability of a thin (L = 1.61 cm) Westerly granite sample under hydrostatic pressures up to 444 MPa. They also analyzed a mathematical model to closely represent their experiment. The partial differential equation for the variation in pressure with x and t in their model was identical to Eq. (1). They assumed that $a^2 \approx 0$ for $\beta \gg \beta_{eff}$ and β_s, and ϕ was small: $\beta = 0.42 \times 10^{-10}$ cm^2/dyn, $\beta_{eff} = 0.025 \times 10^{-10}$ cm^2/dyn, $\beta_s = 0.020 \times 10^{-10}$ cm^2/dyn, and $\phi = 10^{-2}$. They used a reduced form of Eq. (1), $\partial^2 p/\partial x^2 = 0$. This meant that the pressure gradient was constant along the length of the sample, although the gradient would change with time.

To check this approximation, Brace assumed that the entire pore volume v_p in the sample was confined to the middle as shown in Fig. 2. The pressures p_1 in v_1, p_2 in v_2, and p_r in v_p are related through the three differential equations:

$$\left.\begin{aligned} \frac{dp_1}{dt} &= -(p_1 - p_r)(S\, v_R/2v_1) \\ \frac{dv_2}{dt} &= -(p_2 - p_r)(S\, v_R/2v_2) \\ \frac{dp_r}{dt} &= (p_1 + p_2 - 2p_r)(S\, v_R/2v_p) \end{aligned}\right\} \quad (3)$$

where $S = 4k/\beta\mu L^2$, with the initial conditions of $p_1 = p_i$ and $p_2 = p_r = p_0$ at $t = 0$.

Equations (3) have a solution in the form of

$$p_1(t) = p(0,t) = p(x,\infty) + A\, e^{-\gamma t} - B e^{-\alpha t} , \quad (4)$$

where $p(x,\infty)$ is the final pressure, as defined before. A, B, α, and γ are all functions of v_1, v_2, v_p, v_R, k, μ, and β. The porosity of granite is usually small, in the range 0.003

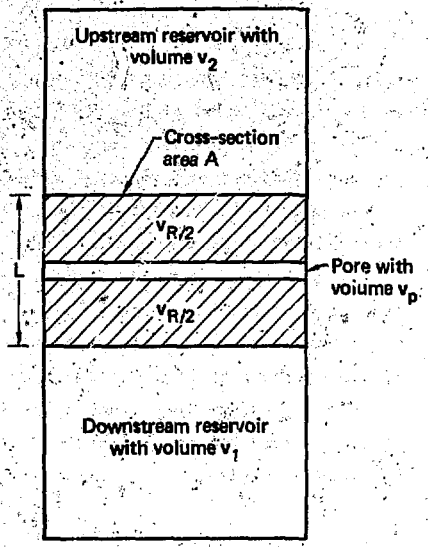

Fig. 2. Schematic diagram of the model of Brace et al.[1] The entire pore volume (v_p) of the rock sample is concentrated at the sample's midsection.

to 0.02; therefore, $v_p \ll v_R$ since $v_p = \phi v_R$. For Brace's calculations, v_R is small enough (8.05 cm^3) that $v_p \ll v_1$ (20 cm^3) and v_2 (5 cm^3), γ is about two orders of magnitude greater than α, and A and B are approximately the same. Equation (4) can be simplified to Brace's equation

$$\frac{(p_1 - p_f)}{(p_0 - p_f)} = \frac{v_2 \exp(-\alpha t)}{(v_1 + v_2)} + \frac{v_p}{4v_1} \exp(-\gamma t) \quad ,$$

where

$$\alpha = \frac{k\mu\, v_R(v_1 + v_2)}{\beta L^2 v_1 v_2} \quad ,$$

$$\gamma = \frac{4k\mu}{\beta L^2 \phi} \quad .$$

This equation simply relates $p_1(t)$ to k. Thus when $v_p \ll v_1$ and v_2, the second term of Eq. (4) decreases much faster with time than the third term. The transient time γ depends upon the permeability of the rock sample. For permeabilities from 10^3 to 1.0 nD, γ is from 3 to 3×10^3 s.

In this simplified model, Brace assumes that the pressure in the pore in uniform, and the pressure gradient is constant along the sample length. Therefore, Eqs. (3) appear to be the consequence of the approximation $a^2 \approx 0$ instead of a check of it. However, the approximation that $a^2 \approx 0$ is not strictly correct. In Table 1, we show values of a^2 as a function of permeability k, using the same values of β, β_{eff}, ϕ, and μ as those used by Brace to calculate a^2.

Table 1. a^2 as a function of permeability k.

a^2, s/cm^2	k, nD
1.61×10^3	1
1.61×10^2	10
1.61×10^1	10^2
1.61	10^3

The approximation $a^2 \approx 0$ is valid only if the measurements are taken after the flow has reached a steady state.

If v_R is large, α and γ in Eq. (4) become similar in value. In our experiments, we are dealing with larger rock samples than Brace's group (660-fold larger) and thus, their simplified equation is no longer valid for our measurements.

Analysis of the Model

From Eq. (1), the characteristic time T_c of the flow is on the order of L^2a^2. This is the time for the fluid moving from v_1 to v_2 to reach its steady state. Table 2 lists the values of the constants shown in Eqs. (1) and (2). These values are appropriate for the samples and apparatus to be used in our study. The calculated values of T_c based on the constants listed in Table 2 are shown in Table 3. The actual time fluid flow reaches a steady state value will be affected by the reservoir volumes through boundary conditions.

Because the problem was complex, we first attempted to work out a general analytical solution by considering only the upstream reservoir. Our purpose here was to ascertain how the upstream reservoir affects variations in fluid pressure at several locations in the sample.

Table 2. Numerical values of the constants used in the calculations.

Constant	Value	Remarks
A	1.824×10^2 cm^2	Fig. 1
L	29.21 cm	Fig. 1
v_1	5, 50, and 500 cm^3	Upstream reservoir volumes
v_2	5, 50, and 500 cm^3	Downstream reservoir volumes
β	0.42×10^{-10} cm^2/dyn	Clark[3]
β_{eff}	0.06×10^{-10} cm^2/dyn	Averaged compressibility of granites at 10 MPa (Brace)[4]
β_s	0.02×10^{-10} cm^2/dyn	Averaged compressibility of granites at 900 MPa (Brace)[4]
μ	1.79×10^{-2} dyn/s/cm^2	Brace et al.[1]
ϕ	0.01	Porosity of Westerly granite (Brace)[4]
k	1 to 10^4 nD	Range of expected permeability

Table 3. Characteristic time T_c as a function of permeability k.

T_c, s	k, nD
6.7×10^6	1
$6. \times 10^5$	10
6.7×10^4	10^2
6.7×10^3	10^3
6.7×10^2	10^4

Laplace transform methods were used to solve Eqs. (1), (2a), and initial conditions:

$$p(x,t) = (p_i - p_0) \times \exp\left(\frac{Aka^2}{v_1\beta\mu}x + \frac{A^2k^2a^2}{v_1^2\beta^2\mu^2}t\right) \times \operatorname{erfc}\left(\frac{ax}{2\sqrt{t}} + \frac{Aka\sqrt{t}}{v_1\beta\mu}\right) + p_0 . \quad (5)$$

The value of p(x,t) is calculated from Eq. (5) by using the numerical values of these variables listed in Table 2.

The results for this calculation are shown in Figs. 3 and 4 for Δp = 2 MPa. Figure 3 illustrates typical linear pressure vs log time plots at several distances from the upstream reservoir. The larger the upstream reservoir volume, the smaller the variation in pressure over time. Figure 4 shows the log pressure vs time plots at x = 0 and v_1 = 50 cm^3 for four values of k. The variations in pressure decrease rapidly with decreasing permeability. From these figures, it is not possible to see when the flow reaches a steady state since the down-

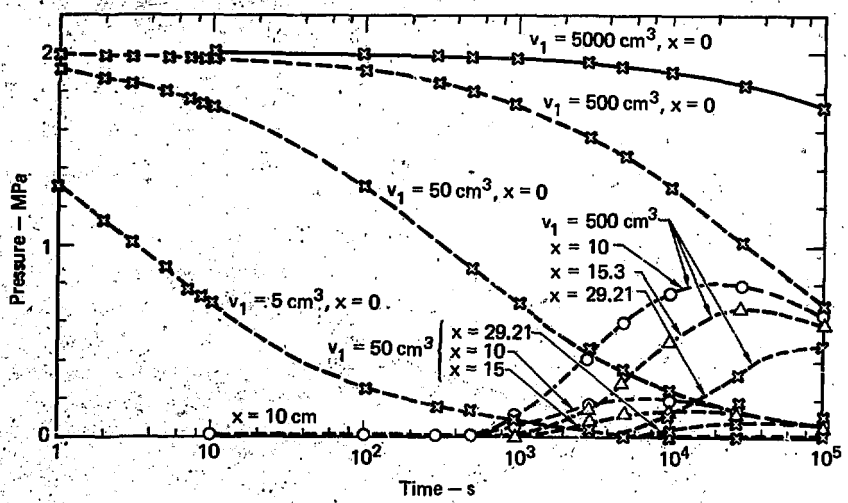

Fig. 3. Analytical solutions of pressures over time at various positions in the sample. x = 0 represents the upstream reservoir, x = 29.21 represents the lower end of the sample. Permeability is 10^2 nD.

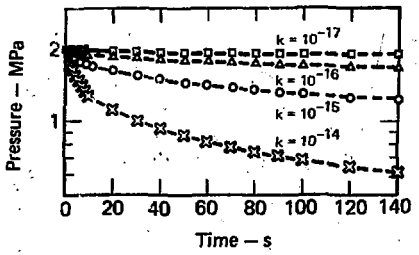

Fig. 4. Analytical solutions of pressure vs time plots in the upstream reservoir as a function of permeability. v_1 = 50 cm^3, x = 0.

stream reservoir was not included in the analyses. However, Fig. 3 shows that for a permeability of 10^2 nD and v_1 = 5 cm^3 (lower left curve), the pressure pulse traverses the sample in about 5 × 10^3 s (83 min).

The next step in arriving at an exact solution to this problem involved adding the influences of the downstream reservoir, v_2. We used the computer code TRUMP[5] to obtain numerical solutions of the variation in pressure for both the upstream and downstream reservoirs over time. In these calculations, we assumed that both the upstream and downstream reservoirs are part of the system, and the boundaries between the reservoirs and the rock sample are part of the interfaces of the system. To simulate actual reservoirs, we used large values for permeability (k = 10^8 D) and porosity (ϕ = 1.0). We also used the values of the constants shown in Table 2 for these calculations. For simplicity, we assumed that the reservoirs have the same cross-section areas as the rock sample. This assumption should not affect the results of our calculations as long as the areas of contact between the sample and the reservoirs are the same as the cross-section areas of the sample. With these assumptions, we made a total of 45 calculations: 3 upstream reservoir volumes, 3 downstream reservoir volumes, and 5 values of permeability. Some of these results are shown in Fig. 5. Comparing Fig. 5 with Fig. 3, we noticed that our numerical results are consistent with our initial analytical results. We also plotted these results on log pressure vs. linear time and log pressure vs. log time scales to see if linear regions would appear. Figures 6 and 7 show some of these plots. Curves in these figures are of similar shape as those in Fig. 5.

The numerical results of our calculations are summarized in Figs. 8 and 9. In Fig. 8, Δp_m is defined as the pressure difference between t = 20 s and ∞ in the upstream reservoir. This 20 s reference time is based upon the observed transient effects due to the temperature increase caused by the sudden pressure increase in the upstream reservoir.[1] Δp_m is the amount of pressure variation available for us to measure within these time limits. In Fig. 9,

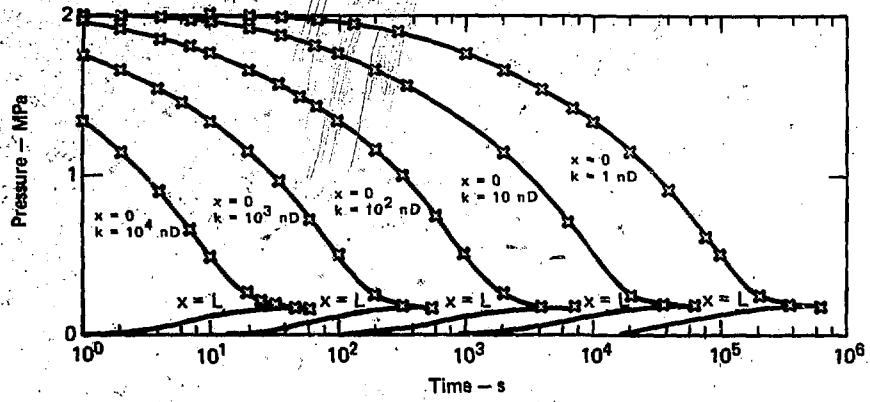

Fig. 5. Numerical solutions of linear pressure vs log time plots at the upstream (x = 0) and downstream reservoir (x = L) at various permeabilities and at v_1 = 50 cm^3, v_2 = 500 cm^3.

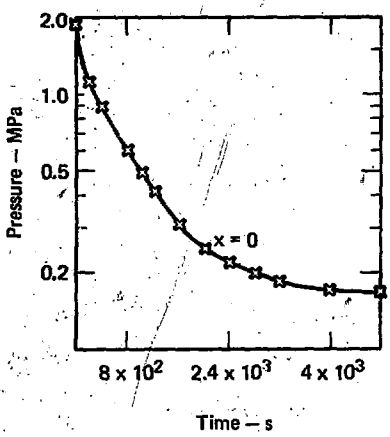

Fig. 6. Numerical solutions of log pressure vs linear time plot of pressure in the upstream reservoir for k = 10^2 nD, and for v_1 = 50 cm^3, v_2 = 500 cm^3.

workable time (T_w) is defined as the time when the pressure in the upstream reservoir is still 0.1 MPa above the final pressure, as shown in Fig. 5. This figure shows the actual time available for us to make effective measurements. A 20 s time mark is shown in Fig. 9.

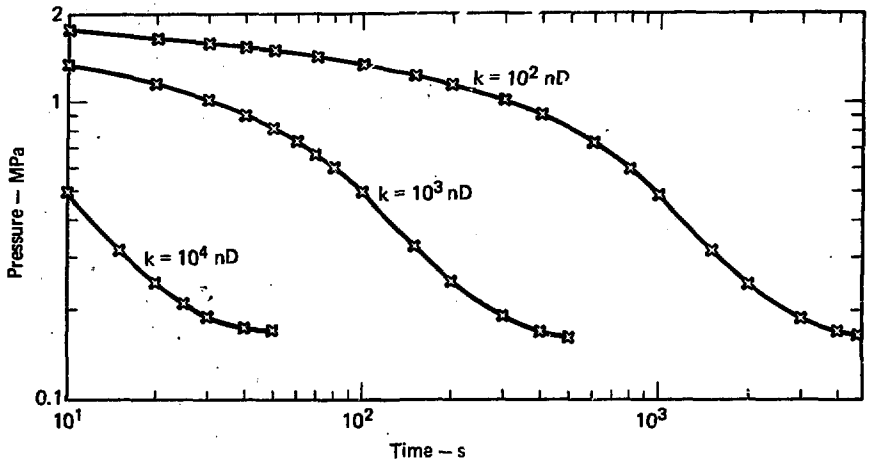

Fig. 7. Numerical solution of log pressure vs log time plots in the upstream reservoir (x = 0) for v_1 = 50 cm^3 and v_2 = 500 cm^3 at various permeabilities.

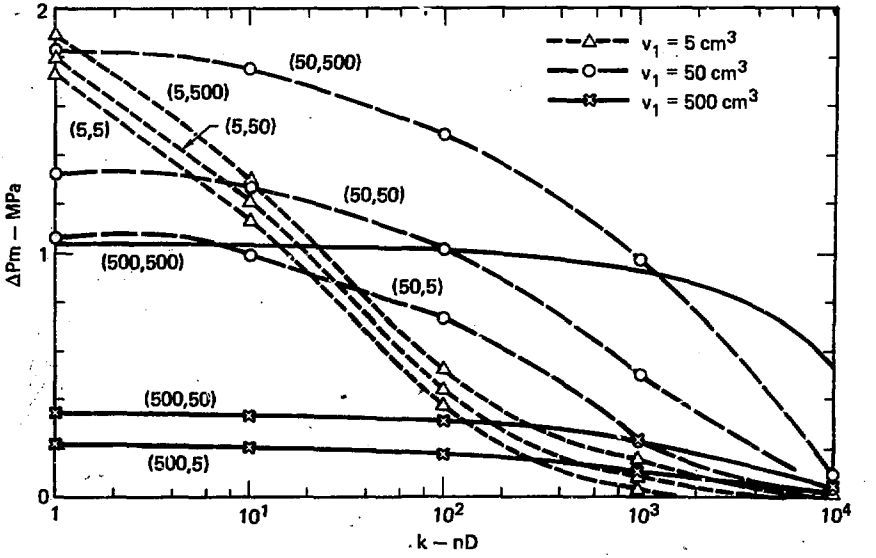

Fig. 8. Pressure difference (Δp_m) vs k at various combinations of v_1 and v_2 (in parenthesis).

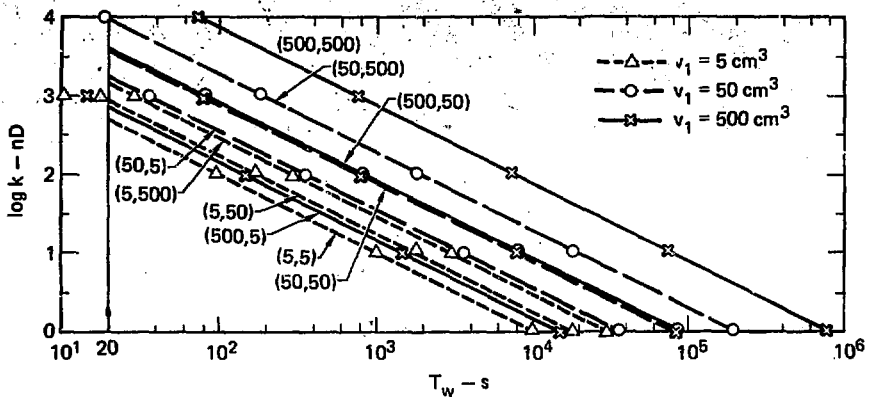

Fig. 9. Log k versus workable time (T_w) at various combinations of v_1 and v_2 (in parenthesis).

Discussions and Conclusions

To select the volumes of the reservoirs, both Δp_m and T_w must be taken into consideration. The pressure difference Δp_m depends upon the final pressure p_f [= $p(x,\infty)$] and the permeability of the sample. Values of the final pressure and the results shown in Figs. 8 and 9 are summarized in Table 4. Note that the smaller the p_f, the larger pressure differences will be. Therefore, v_1 = 5 or 50 cm^3 yield a greater available pressure difference than v_1 = 500 cm^3, if permeability is not considered. From Table 4, for k = 10^4 nD, only the combination of v_1 = 500 cm^3 with v_2 = 500 cm^3 has a significant available pressure difference. The (v_1, v_2) combinations (500, 50) and (500, 5) have only slim margins of Δp_m for the entire permeability range. All of the combinations with v_1 = 5 cm^3 are not suitable for k $\geq 10^3$ nD.

Values for workable time (T_w) in Table 4 show that for k $\geq 10^3$ nD, the (v_1, v_2) combinations (5, 50), (5, 5), and (500, 5) are not suitable for our design. The combinations (5, 500) and (50, 5) allow 10 to 16 s (T_w-20 s) for making measurements, which is too short. For measuring permeability up to 10^3 nD, the following combinations have the greater T_w: (50, 50), (500, 50), (50, 500), and (500, 500).

Taking pressure and time into consideration, we show in Table 5 the optimal combinations of v_1 and v_2 for various permeability ranges. Here,

Table 4. Final pressure (p_f), pressure difference (Δp_m) and workable time (T_w) as functions of v_1, v_2, and k, for Δp = 2.0 MPa. Pressures are in MPa, T_w in s.

Reservoir volume, cm^3			k, 1 nD		k, 10 nD		k, 10^2 nD		k, 10^3 nD		k, 10^4 nD	
v_1	v_2	p_f	Δp_m	T_w	Δp_m	T_w	Δp_m	T_w	Δp_m	T_w	Δp_m	T_w
5	5	0.158	1.731	10^4	1.142	10^3	0.381	10^2	0.032	—[a]	—[a]	—
	50	0.092	1.802	1.7×10^4	1.221	1.7×10^3	0.442	1.7×10^2	0.081	—	—	—
	500	0.018	1.880	3.0×10^4	1.301	3.0×10^3	0.522	3.0×10^2	0.162	3.0×10^1	—	—
50	5	0.924	1.073	3.6×10^4	0.990	3.6×10^3	0.731	3.6×10^2	0.220	3.6×10^1	—	—
	50	0.652	1.331	8.1×10^4	1.272	8.1×10^3	1.002	8.1×10^2	0.501	8.1×10^1	—	—
	500	0.166	1.832	1.8×10^5	1.750	1.8×10^4	1.481	1.8×10^3	0.982	1.8×10^2	0.085	—
500	5	1.791	0.213	1.5×10^4	0.200	1.5×10^3	0.172	1.5×10^2	0.091	—	—	—
	50	1.658	0.341	8.1×10^4	0.321	8.1×10^3	0.312	8.1×10^2	0.220	8.1×10^1	0.020	—
	500	0.949	1.042	7.5×10^5	1.035	7.5×10^4	1.012	7.5×10^3	0.931	7.5×10^2	0.535	7.5×10^1

[a] Δp_m < 0.01 MPa or T_w < 20 s.

Table 5. Optimal combinations of reservoir volumes (v_1 and v_2) as functions of permeability range. Asterisks indicate combinations with $\Delta p_m \geq 0.5$ MPa and $T_w \geq 80$ s.

Reservoir volume, cm^3		Permeability range (k), nD			
v_1	v_2	1-10	$1\text{-}10^2$	$1\text{-}10^3$	$1\text{-}10^4$
5	5	*			
	50	*			
	500	*	*		
50	5	*	*		
	50	*	*	*	
	500	*	*	*	
500	5				
	50				
	500	*	*	*	*

$\Delta p_m \geq 0.5$ MPa and $T_w \geq 80$ s are the conditions considered necessary to collect sufficient data for analysis. The optimal reservoir combinations for $k \leq 10^3$ nD are (50, 50), (50, 500), and (500, 500).

The time scale that we will be using depends upon the rock permeability and the reservior volumes. From our calculations, we estimate that the maximum time for a final pressure to be reached is 10^6 s (>250 h) for k = 1 nD, v_1 = 500 cm^3, and v_2 = 500 cm^3. This is too long to wait between experiments. To speed up the equalizing process after one experiment, we have considered three experimental procedures. In numerically analysing these three procedures, we have assumed that one experiment is completed when the pressure in the upstream reservoir has decreased to 0.1 MPa above the final pressure.

RELAXATION PROCESS

When one experiment is completed, the pressures in both reservoirs are dropped to p_0 or 30 MPa in our analyses. The pressure in the sample is then relaxed to a uniform state in both directions; i.e., the maximum pressure difference in the sample is not detectable (<0.004 MPa). The relaxation time (T_R) depends upon the permeability as well as the reservoir volumes. Table 6 shows the relaxation time for the three optimal pairs of reservoir volumes at k = 1 nD (see also Fig. 11). These are still long

Table 6. *Relaxation time as functions of* v_1 *and* v_2.

v_1, cm^3	v_2, cm^3	T_R, s
50	50	9.2×10^4
50	500	2.23×10^5
500	500	4.01×10^4

periods of time (>11 h). Increasing the permeability by one order of magnitude (e.g., from 1 nD to 10 nD) decreases the T_R by the same order of magnitude (e.g., from 9.2×10^4 to 9.2×10^3 s or 2.6 h).

EQUALIZATION PROCESS

When one experiment is completed, at T = 0 for example (here T, instead of t, is used to represent time in the equalizing process), the pressures in the reservoirs are dropped to p_0' ($p_0' < p_0$). At $T = T_1$, when the pressures in the sample has decreased to a known value, the pressure in the reservoirs are increased to p_1' and p_2' for the upstream and downstream reservoirs, respectively. p_1' and p_2' may not be equal, especially when $v_1 \neq v_2$ but p_1' and p_2' may be equal to or greater than p_0. At $T = T_t$, the pressures in the sample reach a uniform state. Figure 10 illustrates this fall in pressure with time and distance. In this case at T = 0, the pressures in the reservoirs (p_0') are dropped to 28.0 MPa. At $T = T_1 = 1.4 \times 10^3$ s, the pressure in the upstream reservoir is 28.32 MPa, and that in the downstream reservoir is 28.04 MPa. The second cycle is started by increasing the pressure in the upstream reservoir to $p_1' = 30.0$ MPa and the downstream reservoir to $p_2' = 29.88$ MPa. The total time for the equalization process is $T_t = 1.614 \times 10^4$ s. Determinations of p_0', p_1', p_2', and T_1 are empirical and based upon trial and error. Figure 11 illustrates this. For the (500, 500) system, $T_1 = 3.6 \times 10^3$ s with $p_1' = p_2' = 30.25$ MPa is the best combination among these calculations. For the (50, 500) system, $T_1 = 1.4 \times 10^3$ s, $p_1' = 30.0$ MPa with $p_2' = 29.88$ MPa is the best combination. For the (50, 50) system, $T_1 = 5.0 \times 10^3$ s with $p_1' = p_2' = 30.0$ MPa the best. Figure 11 also illustrates that the equalization procedure is not necessarily better than the relaxation process. These best combinations, however, have a T_t smaller than that in the corresponding relaxation procedure. The equalization time for the small permeability (k = 1 nD) sample is still about 10^4 s, which is 2.8 h.

RELEASING CONFINING PRESSURE

We may also use either the relaxation or equalization processes along with a release of confining pressure.

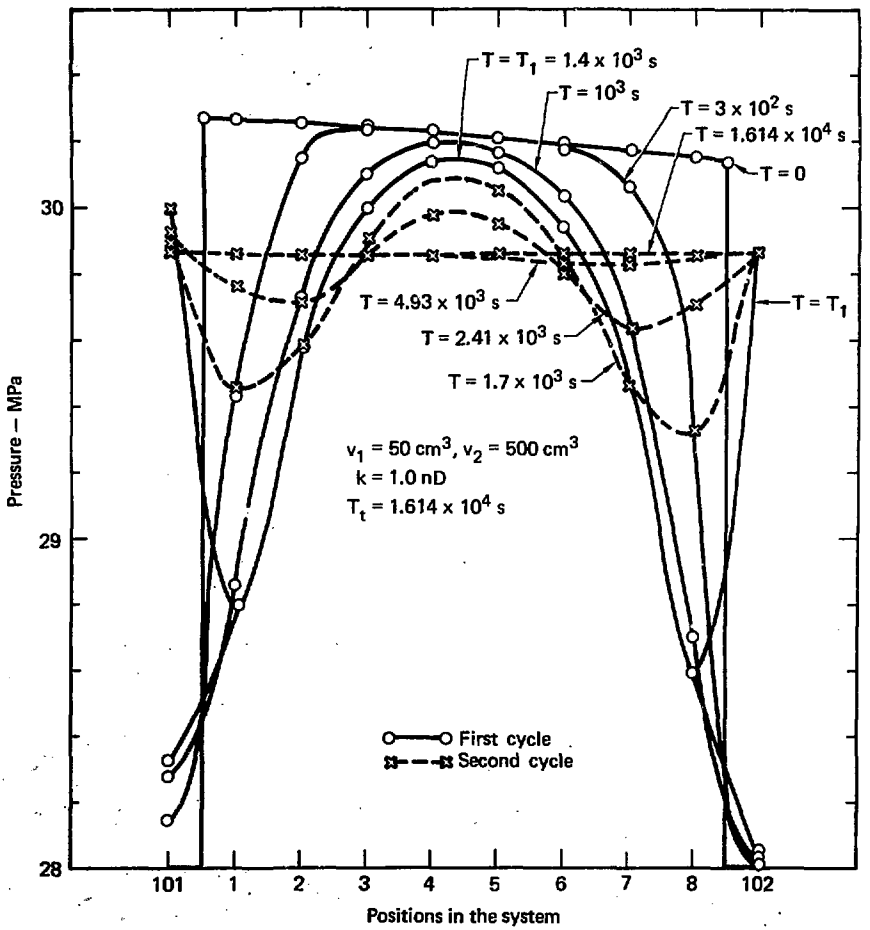

Fig. 10. Pressure variations in the system over time. System positions 101 and 102 are the upstream and downstream reservoirs, respectively.

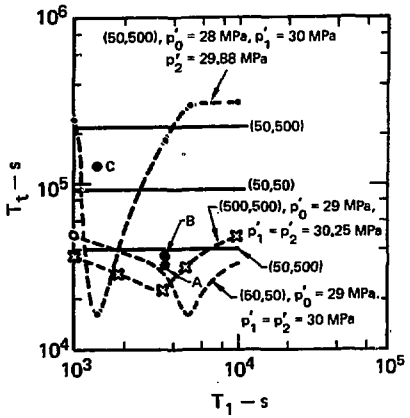

Fig. 11. Total time (T_t) of the equalization process as a function of middle time (T_1). Solid lines are relaxation times (Table 6).

A is for (500, 500) system, p_0' = 29 MPa, p_1' = p_2' = 30 MPa.
B is for (500, 500) system, p_0' = 29 MPa, p_1' = p_2' = 30.5 MPa.
C is for (50, 500) system, p_0' = 28 MPa, p_1' = p_2' = 30 MPa.

v_1 and v_2 are in parenthesis. The dashed lines are arbitrary, only to connect data points. k = 10^{-9} D.

If the sample originally has a low permeability (i.e., not due to the increased confining pressure), we may have to accept a slow process. If low permeability of the sample is due to the increase in confining pressure, then we may be able to reduce the equalization time significantly by reducing the confining pressure to increase permeability. As indicated in the relaxation process, increasing the permeability from 1 nD to 10 nD reduces t by one order of magnitude, to be within one hour. The amount of confining pressure that must be released to achieve this increment in permeability depends upon the individual rock sample; this increase may be significant since, in the smaller permeability range, permeability tends to vary slowly with pressure.[1] Releasing confining pressure during an experiment may produce nonuniform and incoherent deformation of the jacket on the sample and disturb other measurements that depend on jacket contact. This problem may be eased by using thin and soft jackets, and releasing the confining pressure slowly.

Acknowledgments

The author would like to thank D. Montan for his help in running the TRUMP code. Discussions with D. Trimmer and H. Heard were very helpful.

References

1. W. F. Brace, J. B. Walsh, and W. T. Frangos, "Permeability of Granite Under High Pressure," *J. Geophys. Res.* 73, 2225 (1968).
2. D. Trimmer, Lawrence Livermore Laboratory, Livermore, Calif., private communication (June, 1977).
3. S. P. Clark, Jr., Handbook of Physical Constants (Geological Society of America, Membership 97, New York, N.Y., 1966), p. 485.
4. W. F. Brace, "Some New Measurements of Linear Compressibility of Rocks," *J. Geophys. Res.* 70, 391 (1965).
5. A. L. Edwards, *TRUMP: A Computer Program for Transient and Steady-State Temperature Distributions in Multidimentional Systems*, Lawrence Livermore Laboratory, Livermore, Calif., UCRL-14754, Rev. 3 (1972).

CD/ml/vt,mg/jf